

Analysis of Shape Distortions in Sessile Drops

G. McHale,^{*,†} H. Y. Erbil,[‡] M. I. Newton,[†] and S. Natterer[†]

Department of Chemistry and Physics, The Nottingham Trent University, Clifton Lane, Nottingham NG11 8NS, United Kingdom, and Kocaeli University, Faculty of Sciences and Arts, Department of Chemistry, 41430 Izmit, Kocaeli, Turkey

Received March 28, 2001. In Final Form: July 16, 2001

The effects of drop flattening and substrate surface heterogeneity on the cross-sectional and planar shapes of droplets of liquids resting on solid surfaces are examined. A simple method, volume single image sequencing, for examining a side view digital image profile is developed. Advantages of this sequential approach are that the influence of the finite pixel resolution is made explicit and the confidence with which shape deviations can be deduced can be quantified. A dual-camera video microscopy system was developed for simultaneously recording the planar and side views of sessile drops. Experimentally observed profiles have been analyzed for large and small drops of triply distilled water evaporating from poly(ethylene terephthalate) (Mylar), poly(methyl methacrylate), Teflon, and glass substrates. The planar view shows that deviations from a circular shape often occur in the latter stages of evaporation but that these are not apparent from a side view observation of the droplet. Experiments were conducted with drops of glycerine on a grooved glass substrate with side view observations both along and at 90° to the axis of the grooves. Two side views were also used with drops of glycerine on Mylar and Teflon, and this demonstrated the large variation in measured contact angle possible dependent upon the direction of the side view.

Introduction

The measurement of a contact angle, θ , provides information on the interaction of a liquid with a solid through Young's equation, $\gamma_{SV} = \gamma_{SL} + \gamma_{LV} \cos \theta$, where the γ_{ij} 's are the interfacial tensions.^{1,2} A range of methods exist to measure the contact angle, and one of the most frequently used is to observe the side profile of a small droplet resting on the solid surface. The droplet is small so that the relative importance of gravity to capillary forces is diminished; the characteristic dimension is the capillary length $\kappa^{-1} = (\gamma_{LV}/\rho g)^{1/2}$, where ρ is the density of the liquid and g is the acceleration due to gravity. When a contact angle is measured using a side profile view, the assumption made, either implicitly or explicitly, is that the drop has an axisymmetric drop shape. In the simplest case, gravity is ignored and the theoretical drop shape is that of a spherical cap.^{3–5} A more complex analysis is to assume an ellipsoidal cap as a model of a drop with a slight flattening due to gravity.⁶ An alternative method that claims an extremely high accuracy, axisymmetric drop shape analysis (ADSA-P), uses a numerical solution to the equation for the excess Laplace pressure including a gravitational term.^{7,8} However, even in this method an accurate determination of the drop shape does not guarantee an

accurate contact angle measurement unless the location of the solid surface can be determined accurately. This baseline is usually identified from the point where the drop profile meets its reflection in the substrate. In practice, contact angles reported for a given system often cover a wide range of values. Contact angle hysteresis can be due to a range of chemical and physical causes, including surface roughness, surface restructuring, diffusion of liquid into solids, surface contamination, and local surface adsorption.⁹

In contact angle measurement, it is not simply the determination of an angle that is important but also the extent with which confidence can be assigned to that particular measurement. Side views of sessile drops are frequently used to determine contact angles, but the shape information contained within an image is rarely examined for indications that nonaxisymmetry or other drop shape distortions are occurring. In ADSA-P, for example, any deviations from a spherical cap profile are effectively accounted for by the gravitational term even though they may originate from substrate heterogeneity. In a previous report, we examined how a sequence of subprofiles can be constructed from a single image to provide a trend in a drop shape and a quantification of contact angle accuracy (single image sequencing, SIS).¹⁰ A particular realization of this idea, volume single image sequencing (V-SIS), based upon the volume in an axisymmetric ellipsoidal drop shape was presented, and comparisons to simulations were performed. It was shown that a small baseline error could lead to a small systematic change in the measured contact angle for different size drops, thus giving a small apparent drop volume dependence for the contact angle.

In this report, we further develop the V-SIS method so that it provides both under- and overestimates bracketing the true values of the contact angle and drop shape parameter. The method is then applied to experimental

* Corresponding author. E-mail: glen.mchale@ntu.ac.uk. Tel: +44 (0)115 8483383. Fax: +44 (0)115 9486636.

[†] Nottingham Trent University.

[‡] Kocaeli University.

(1) Adamson, A. W. *Physical Chemistry of Surfaces*; Wiley: New York, 1976.

(2) Léger, L.; Joanny, J. F. *Rep. Prog. Phys.* **1992**, *55*, 431–486.

(3) Picknett, R. G.; Bexon, R. *J. Colloid Interface Sci.* **1977**, *61*, 336–350.

(4) Bourges-Monnier, C.; Shanahan, M. E. R. *Langmuir* **1995**, *11*, 2820–2829.

(5) Rowan, S. M.; Newton, M. I.; McHale, G. *J. Phys. Chem.* **1995**, *99*, 13268–13271.

(6) Erbil, H. Y.; Meric, R. A. *J. Phys. Chem.* **1997**, *B101*, 6867–6873.

(7) Rotenburg, Y.; Boruvka, I.; Neumann, A. W. *J. Colloid Interface Sci.* **1983**, *93*, 169–183.

(8) Li, D.; Cheng, P.; Neumann, A. W. *Adv. Colloid Interface Sci.* **1992**, *39*, 347–382.

(9) Shanahan, M. E. R. *Macromol. Symp.* **1996**, *101*, 463–470.

(10) Erbil, H. Y.; McHale, G.; Rowan, S. M.; Newton, M. I. *J. Adhes. Sci. Technol.* **1999**, *13*, 1375–1391.

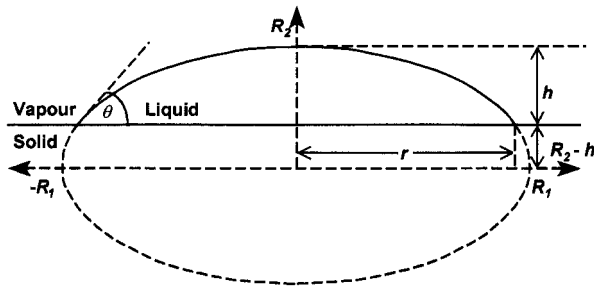


Figure 1. A drop with a fitted ellipsoidal cap profile showing global parameters R_1 and R_2 and local parameters h , r , and θ .

results using sessile drops with both static and dynamic contact angles. An experimental system was set up to enable simultaneous video recording of both planar and side views of the drops, so that the symmetry, axial or otherwise, could be determined. The experiments included evaporation of large (i.e., contact radius comparable to the capillary length) and small drops of water from Mylar, poly(methyl methacrylate) (PMMA), Teflon, and glass substrates and of organic liquids from Teflon. To further investigate the influence of surface heterogeneity, we also performed experiments using drops of glycerine on grooved glass surfaces and on Mylar and Teflon. In these latter cases, the drops are nonvolatile and we therefore made side view observations of each drop along two directions separated by 90° . In the case of the grooved glass surface, these directions were along and at 90° to the direction of the grooves.

Volume Single Image Sequencing

A digital representation of the profile of a sessile drop is necessarily limited in accuracy by the pixel resolution of the captured image. One idea of a single image sequence is to make this quantization apparent in the analysis and so enable its influence on the accuracy of the final contact angle to be quantified. Single image sequencing also builds upon the idea that a drop shape has two distinct types of parameters: global and local.¹⁰ A global parameter is one that does not depend on the location of the supporting solid surface. For example, if the drop shape is a spherical cap then the spherical radius is a global parameter as it could be determined from any portion of the profile without requiring information about the location of the solid surface. In contrast, the contact angle is a local parameter as it depends on the precise location of the supporting solid surface as well as the curvature of the liquid–vapor interface. In single image sequencing, the image is progressively examined from its apex down toward the substrate. In effect, an imaginary baseline is moved downward one pixel row at a time, and on each move, estimates of the local and global parameters are created. Once the pixel resolution becomes unimportant, the global parameters should become constant. When the imaginary baseline corresponds to the true baseline, a contact angle estimate is obtained, but because it is the limit of a sequence of estimates, its sensitivity to the precise location of the baseline should be apparent.

Volume single image sequencing is one particular implementation of the SIS idea. In V-SIS, we assume the drop shape is an axisymmetric ellipsoidal cap (Figure 1); this is a first approximation to a deviation in shape from a spherical cap. The contact angle, θ , can be determined from measurements of the drop height, h , the contact

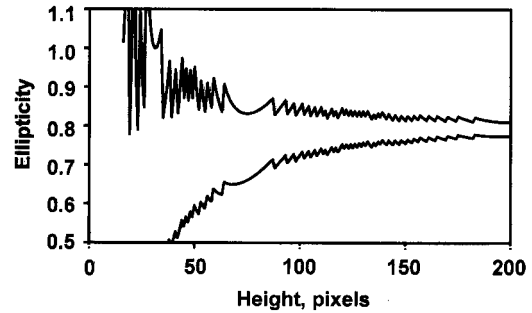


Figure 2. Volume single image sequence for the ellipticity determined from a simulation of a slightly flattened sessile drop. The upper curve is the overestimate, and the lower curve is the underestimate.

radius, r , and the ellipticity, ϵ_r :

$$\theta(h, r, \epsilon_r) = \arctan\left(\frac{2hr}{r^2 - \left(\frac{h}{\epsilon_r}\right)^2}\right) \quad (1)$$

The ellipticity is a global parameter and is the ratio $\epsilon_r = R_2/R_1$ where R_2 is the minor axis and R_1 is the major axis of the ellipse describing the drop profile; $\epsilon_r = 1$ for a circular shape and $\epsilon_r < 1$ for a flattened shape. In the drop volume method, the ellipticity is given from the drop volume, V , by

$$\epsilon_r(h, V, r) = \left(\frac{\pi h^3}{6V - 3\pi h r^2}\right)^{1/2} \quad (2)$$

The drop height, contact radius, and volume are all accessible from a digitized profile image. Assuming axisymmetry, the volume can be estimated from

$$V_a = \pi \sum_{p=\text{rows}} r_p^2 \quad (3)$$

One further complication with all digital images is that a pixel does not represent a point in physical space but is a length. Thus, all distances measured from an image have an experimental accuracy of ± 1 pixel. In our implementation of V-SIS, we measure r_p and h_p for each subimage and construct an overestimate and an underestimate for V_a , ϵ_r , and θ using eqs 1–3. To create these overestimates and underestimates, we first threshold the image and label the pixel rows starting with $h = 1$ for the pixel row at the apex of the drop, and the maximum and minimum heights, h_{\max} and h_{\min} , are given by $(h \pm 1/2)$, respectively. The minimum radius of a row, r_{\min} , is one-half of the number of pixels within the row in the thresholded drop image, and the maximum radius, r_{\max} , is 1 pixel greater. The overestimates of the ellipticity and the contact angle are then calculated using $\epsilon_r^{\max} = \epsilon_r(V_{\min}, r_{\max}, h_{\max})$ and $\theta^{\max} = \theta(h_{\max}, r_{\max}, \epsilon_r^{\min})$, respectively. Similarly, the underestimates of the ellipticity and the contact angle are then calculated using $\epsilon_r^{\min} = \epsilon_r(V_{\max}, r_{\min}, h_{\min})$ and $\theta^{\min} = \theta(h_{\min}, r_{\min}, \epsilon_r^{\max})$, respectively. Our simulations show that the true ellipticity and contact angle can be at either of these extremes and is not simply an average of the two estimates. An example simulation is given in Figure 2. The effect of the finite pixel resolution is evident from the nonconstant value and error range of the ellipticity when the height is small. The small sawtooth oscillations which continue once the ellipticity value has saturated to a constant are also due to the finite pixel resolution.

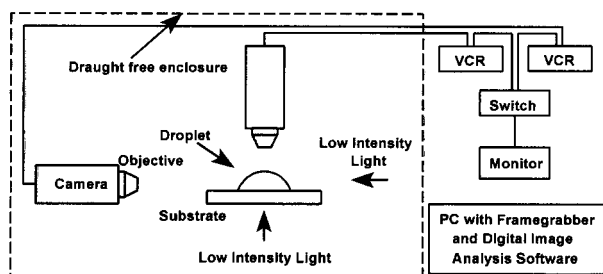


Figure 3. Experimental arrangement for simultaneous planar and side view video microscopy of sessile drops.

Experimental Method

The experimental system (shown in Figure 3) incorporated two cameras, one mounted horizontally and the other vertically, with both equipped with microscope objectives and adjustable vernier stages. Each camera was connected to a video recorder, and a real-time display of either image was provided on a monitor via a switch box. The substrates were placed on an adjustable horizontal platform, and droplets of liquid were deposited from a syringe. Low-intensity light sources were placed behind and above/below the droplets. The cameras, light sources, substrate, and syringe were contained within a chamber housing to shield the droplets from air currents within the laboratory. The temperature and relative humidity within this chamber were monitored. The recorded images were converted into a digital format using a Data Translation DT3152 scientific framegrabber card. Calibration images were captured to convert pixel distances to real-world distances for each magnification and to check for optical distortions. This system was capable of recording 25 frames per second with image resolutions of 769×576 and a one-to-one aspect ratio for both the planar and side profile views. Initial image processing was performed using the UTHSCSA ImageTool program together with in-house routines to extract the profiles and perform the V-SIS analysis.

Two types of experiments were conducted with the system. In the first case, we monitored the evaporation of triply distilled water from Mylar, PMMA, Teflon, and glass substrates and the evaporation of organic liquids (octane, nonane, decane, *n*-butanol, and toluene) from Teflon. Drop sizes varied from ones with contact diameters comparable to the capillary length of water (~ 2.8 mm) to ones of around one-fifth this size. The intention in these experiments was threefold: first, to observe how the asymmetry, as judged from the planar view, was correlated with the drop shape viewed from the side; second, to determine whether drops became more axisymmetric as their size reduced during evaporation; third, to assess the effectiveness of the V-SIS technique with a range of contact angles and drop sizes. To further investigate the relationship between a side view and an asymmetry in a drop, we performed a second type of experiment using a substrate with a known asymmetry. In this case, a glass surface with shallow regular grooves (a diffraction grating) was used with drops of glycerine. This provided drops with stable contact angles and a controlled asymmetry due to the enhanced spreading along the direction of the grooves. As the drops were nonvolatile, we were able to take side view images along the two directions parallel and perpendicular to the grooves, in addition to the planar view. For comparison, we also deposited glycerine drops on Mylar and PMMA substrates and viewed these drops in side profile along two orthogonal directions. Substrates were thoroughly cleaned in ethyl alcohol, wiped with a cloth containing dilute soap solution, rinsed in distilled water, and dried in an oven.

Results and Discussion

One of the first observations arising from the experimental system's ability to provide simultaneous views from both above and from the side is that drops with quite strong and evident asymmetry when viewed from above can present side profile images which appear to conform to good quality spherical cap, or slightly flattened spherical cap, shapes. An apparently undistorted side profile image is therefore no guarantee that significant drop shape

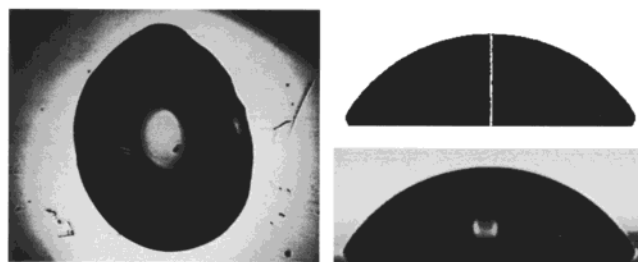


Figure 4. Comparison of simultaneous planar and side views of a drop of water evaporating from a Mylar substrate. The black and white image in the upper right corner is the side view obtained by thresholding the side view image; the central white line is the center location between the two sides of the drop for each row.

distortions are not occurring around the drop perimeter. Figure 4 shows an example of a distorted water drop on Mylar. The left image is the top view, and the lower right is a simultaneous side profile view. The upper right image shows the effect of thresholding the image and creating a center line by setting to white the center location between the two edges for each row. Analyzing the side profile image on the assumption of axisymmetry gives an apparently good spherical cap drop shape with an ellipticity of (0.97 ± 0.05) and a contact angle of $(59.3 \pm 2.4)^\circ$. On some substrates, a smaller drop, but with a contact angle in excess of 30° so that it is not in the film regime, is more strongly influenced by heterogeneities of the surface. The drop size compared to the capillary length is not then a reliable indicator of axisymmetry. This is particularly important because commercial contact angle systems using sessile drops often rely solely on a side profile image of a small drop.

The increasing influence of surface heterogeneity as a drop's size reduces was confirmed in the evaporation experiments. Drops did not necessarily become more axisymmetric as they evaporated, although usually this did occur when a contact line depinned and the contact radius started to contract. In previously published studies of evaporation, side profile views of drops were used and the drop shape was modeled as a spherical^{3,4,11,12} or an ellipsoidal cap.¹³ The motivation in the modeling was to allow for a drop flattening caused by gravity.⁶ Alternative possibilities for drops adopting a flattened profile include internal flows driven by the evaporative flux occurring at the contact line,¹⁰ solute deposition and self-pinning at the contact line,^{14,15} or evaporatively induced variations in interfacial tensions.¹⁶ A slight drop flattening may be an indication of surface heterogeneity and nonaxisymmetry in the drop shape, rather than simply a gravitational effect. The shape determined from a side view profile may then be of use in providing confidence in the contact angle determined from the image.

Figure 5 shows an example of the drop shape for glycerine on a grooved glass surface. The top view shows the expected elongation along the direction of the grooves, and the side views show the cross-sectional shapes from two orthogonal directions across and along the direction

(11) Birdi, K. S.; Vu, D. T.; Winter, A. *J. Phys. Chem.* **1989**, *93*, 3702–3703.

(12) McHale, G.; Rowan, S. M.; Newton, M. I.; Banerjee, M. K. *J. Phys. Chem.* **1998**, *B102*, 1964–1967.

(13) Meric, R. A.; Erbil, H. Y. *Langmuir* **1998**, *14*, 1915–1920.

(14) Deegan, R. D.; Bakajin, O.; DuPont, T. F.; Huber, G.; Nagel, S. R.; Witten, T. A. *Nature* **1997**, *389*, 827–829.

(15) Deegan, R. D. *Phys. Rev. E* **2000**, *61*, 475–485.

(16) Durbin, D. Interfacial phenomena occurring in drying surfactant droplets and polymer latex films. Ph.D. Thesis, Lehigh University, Bethlehem, PA, 1981.

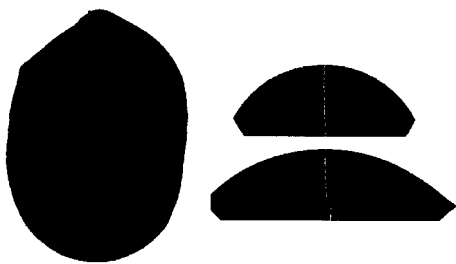


Figure 5. Top and side view profiles of a drop of glycerine on a grooved glass surface. The top view shows a clear elongation along the direction of the grooves, while the two side profiles, along and at 90° to the axis of the grooves, both show a slightly flattened profile.

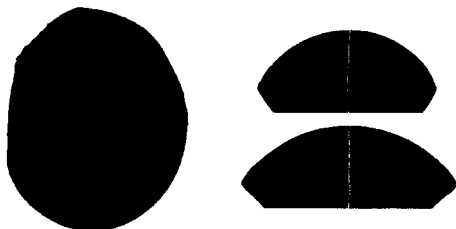


Figure 6. Top and side view profiles of a nonaxisymmetric drop of glycerine on a Mylar surface. The top view shows some asymmetry, but the two side views in directions mutually at 90° show little evidence of the asymmetry.

defined by the grooves. The side view profiles show the beginning of the drop reflection in the substrate. The contact angles and ellipticities are $(62.9 \pm 3.5)^\circ$ and (0.97 ± 0.10) and $(46.9 \pm 2.4)^\circ$ and (1.08 ± 0.18) , for viewing directions along and at 90° to the grooves. The grooved surface provides a clear and systematic asymmetry in drop shape and so provides a large variation in the side view determined contact angles. However, we also found large variations in the measured contact angle for glycerine deposited on Mylar and PMMA when the top view showed some asymmetry. In these cases, the side profile views did not always show clear indications of the asymmetry. Figure 6 shows an example for glycerine on Mylar. The top view shows clear asymmetry, but this is not immediately apparent from either of the side views. The contact angles and ellipticities deduced from these two viewing directions, which are separated by 90°, are $(68.7 \pm 3.2)^\circ$ and (0.911 ± 0.065) and $(57.2 \pm 2.5)^\circ$ and (0.96 ± 0.10) . The asymmetry in the side view is reflected in the V-SIS analysis by a smaller value for the ellipticity. In the studies of nonaxisymmetric drops of glycerine, it appears that in a side profile view where the contact diameter is smaller, the contact angle is higher. In the majority of these cases, the ellipticity was found to be less than unity.

Different methods can be applied to estimate drop shape from a side view profile. However, in all cases, it is important to accurately locate the baseline in the image representing the substrate surface. In the V-SIS technique, a clear change in the trend of the ellipticity and contact angle occurs when the reflected part of the profile is included in the sequence (Figure 7). In Figure 7, the change in trend occurs at a pixel height of 188 and gives an ellipticity of (0.98 ± 0.04) with a contact angle of $(69.5 \pm 1.7)^\circ$. This change in trend helps identify the baseline and quantifies the sensitivity of a contact angle determination

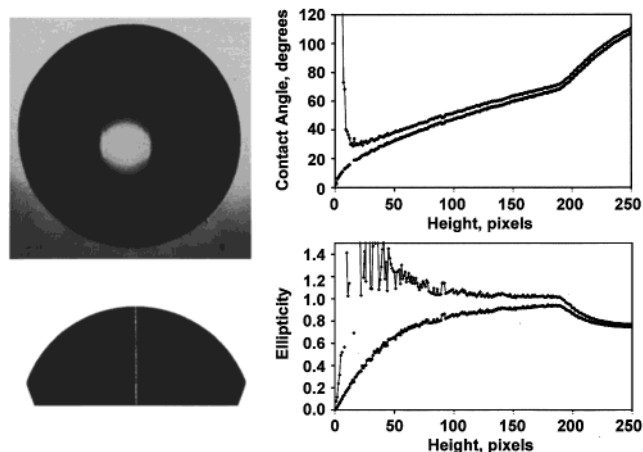


Figure 7. Top and side views and the ellipticity and contact angle deduced using the V-SIS technique for a water drop on Mylar. A clear change in trend occurs at a pixel height of 188 as the reflected part of the profile is included in the sequence.

to the precise location of the baseline. The sawtooth trend due to the pixel resolution is evident in the images and helps quantify the accuracy of the contact angle. The V-SIS technique can be used to determine contact angles over a wide range of angles, but in our studies we found that a precise determination of ellipticity was difficult when a drop had a low contact angle ($<40^\circ$). This is because a lower contact angle provides a profile image with a smaller portion of the overall ellipse being considered.

Conclusion

A shape analysis technique, volume single image sequencing (V-SIS), has been developed and applied to drop shape determination from side view profiles of sessile drops. A simultaneous side and planar view video microscopy system has been developed and used to examine the relationship between contact angle and drop shape and the relationship between the drop ellipticity and drop asymmetry. A sequence of experiments has been performed following the evaporation of drops of water and organic liquids from glass and polymer surfaces. Some drops showing clear nonaxisymmetry when viewed from above were found to provide apparently good side view profiles with only a slight flattening from a spherical cap shape. As drops evaporated and reduced in size, an increase in drop asymmetry was observed in some cases, and this was attributed to surface heterogeneity. In these cases, a small drop size compared to the capillary length is not a good indicator of drop axisymmetry. Complementary experiments were performed with two orthogonal side profile views of drops of glycerine on Mylar, PMMA, and grooved glass surfaces. These experiments further confirmed that side view profiles of a drop could provide apparently good symmetric side view profiles conforming to an approximate spherical cap, while the planar view of the drop showed clear and strong asymmetry.

Acknowledgment. G.M. and H.Y.E. acknowledge the support of The Royal Society and TÜBİTAK under a European Science Exchange Project.

LA010476B